Geofísica Internacional
ISSN: 0016-7169
silvia@geofisica.unam.mx
Universidad Nacional Autónoma de México
México

Flores-Morales, A. L.; Parés-Sierra, A.; Marinone, S. G.
Factors that modulate the seasonal variability of the sea surface temperature of the Eastern Tropical Pacific
Geofísica Internacional, vol. 48, núm. 3, julio-septiembre, 2009, pp. 337-349
Universidad Nacional Autónoma de México
Distrito Federal, México

Geofísica Internacional 48 (3), 337-349 (2009)

Factors that modulate the seasonal variability of the sea surface temperature of the Eastern Tropical Pacific

A. L. Flores-Morales*, A. Parés-Sierra and S. G. Marinone
Departamento de Oceanografía Física, Centro de Investigación Científica y Educación Superior de Ensenada, Ensenada, B. C., Mexico.

Received: June 12, 2008; accepted: May 13, 2009

Resumen

Se estudiaron los principales factores que modulan la variabilidad estacional de la temperatura superficial del mar (TSM) en el Pacífico Tropical Oriental. Para ello se analizaron las siguientes bases de datos: TSM y viento de la base Comprehensive Ocean–Atmosphere Data Set de 1978 a 1997, campos climatológicos de temperatura y salinidad de LEVITUS y alturas del nivel del mar de los altímetros TOPEX/Poseidon de 1993 a 2002. Como factores locales importantes que modulan esta variabilidad se identificaron: (1) la influencia del Golfo de California junto con el desplazamiento estacional de la Corriente de California, que se extiende desde la boca del Golfo hacia el sur y oeste unos 200 km y por el lado occidental de la península de Baja California hacia el norte aproximadamente 300 km; (2) la influencia del Golfo de Tehuantepec y del Golfo de Papagayo, donde, debido al comportamiento de los vientos, se genera un enfriamiento local de la superficie durante el invierno; (3) surgencias en el Ecuador, frente a Cabo Corrientes y frente a las costas de Baja California; (4) la variación espacial y temporal de la Zona de Convergencia Intertropical y su relación con el ecuador térmico; (5) la propagación de señales remotas y (6) la variación estacional del sistema de corrientes ecuatoriales.

Palabras clave: Pacífico Tropical Oriental, temperatura superficial del mar, zona de convergencia intertropical, surgencias, sistema de corrientes ecuatoriales.

Abstract

Seasonal variability of the sea surface temperature (SST) in the Eastern Tropical Pacific were studied. For this purpose the following data were analyzed: SST and wind data from the Comprehensive Ocean–Atmosphere Data Set from 1978 to 1997, temperature and salinity fields from the LEVITUS climatology and sea surfac heights from TOPEX/Poseidon from 1993 to 2002. Various locally important factors that modulate this variability were identified: (1) the influence of the Gulf of California with the seasonal variability of the California Current, which extend about 200 km from the mouth towards the south and west, and about 300 km from the peninsula's west side toward the north; (2) the influence of the Gulfs of Tehuantepec and Papagayo where, due to the behavior of the winds, a local cooling of the surface during winter is generated; (3) upwelling at the Equator, off Cabo Corrientes, and off the west coast of Baja California; (4) spatial and temporal variation of the Inter-Tropical Convergence Zone and its relation with the thermal equator; (5) remote propagating signals in the zone; and (6) seasonal variations of the Equatorial Current System.

Key words: Eastern Tropical Pacific, sea surface temperature, wind, intertropical convergence zone, upwelling, equatorial current system.

Introduction

Solar radiation dictates the average and seasonal variability of the sea surface temperature (SST). Local effects due to the bathymetry, local variations in the wind forcing and the circulation, modify the temperature patterns. In this study we examine the factors that modify the basic form of the seasonal variability of SST in a region of the Eastern Tropical Pacific (ETP).

In the ETP there is a region where the SST is warmer than 28.5°C throughout the year. This area, known as the Eastern Pacific Warm Pool (EPWP), extends in a belt that goes from 6° N to 15° N and from approximately 120° eastward to the Mexican coast (Fig. 1a). The EPWP is part of the Western Hemisphere Warm Pool, which begins to develop in the northeastern tropical Pacific in early spring. This pool is of great importance because it helps to modulate the weather in Mexico and part of The United States of America by its high atmospheric convection. It is also a reservoir of heat and moisture for the monsoon circulation over Central America (Magaña, *et al*, 1999; Wang and Enfield, 2001, 2003; Magaña and Caetaño, 2005; Amador *et al*., 2006).

The SST in the tropical Pacific during average conditions is usually between 6° and 8°C higher in the west than in the east. This disparity is due to the fact that the trade winds blow typically toward the west in the equatorial belt, generating upwelling of cold water along the equator and off the South American coast. During "El Niño" conditions, the trade winds weaken or reverse their direction and SST values above normal are observed in the east and central equatorial Pacific Ocean (Philander, 1990).

SST variability as well as the circulation of the ETP is greatly influenced by the variability of the winds that generally blow toward the equator along the coast (Badan-Dangon, 1998). This is also the case with the California Current System (CCS): its seasonal variations are strongly controlled by the variation of the wind (Parés-Sierra *et al*., 1997).

An important and well-known factor that modifies the basic distribution of SST in the ocean is upwelling. This phenomenon occurs mainly around the equator and along the occidental coasts of continents, where winds move the surface water away from the coast or the equator, replacing it with cold thermocline and subthermocline water rich in nutrients, thus altering the SST and the productivity. This is certainly the case for some parts of the ETP, specially its northern part, along the Baja California Peninsula (Parés-Sierra *et al*, 1997; Fielder and Talley, 2006). In contrast, for the southern part, the absence of consistent upwelling-favorable winds makes the region much less productive (Trasviña and Barton, 1997).

The topography of southern Mexico is dominated by the Sierra Madre del Sur range, which averages 2000 m above sea level. This range is interrupted by a gap approximately 40 km width know as "Paso de Chivela" which, through its channeling effect, allows strong winds (during winter months) to cross the continent from the north (Gulf of Mexico, Fig 1a). These winds are known as "Nortes" (Alvarez *et al*. 1989; Trasviña *et al*. 1995; Romero-Centeno *et al*. 2003); a similar situation occurs in the Gulf of Papagayo where, in some cases, SST anomalies that propagate westward as gyres are produced (Stumpf and Legeckis 1977, Fig 1a).

Another potentially important factor of SST modulation in the zone seems to be the connection between low-frequency signals from the equatorial Pacific and the northeast Pacific (Enfield and Allen, 1980; Parés-Sierra and O'Brien, 1989; Clarke and Van Gorder, 1994).

The objective of this study is to document the seasonal variability of SST and the factors that affect/modulate this variability in the ETP. Even though most of the phenomena mentioned in this article are known and have been presented elsewhere, a novel approach in quantifying some causal relationship (i.e. sea surface temperature-wind-sea surface height) is presented. Also the information is integrated in the context of the Mexican Pacific.

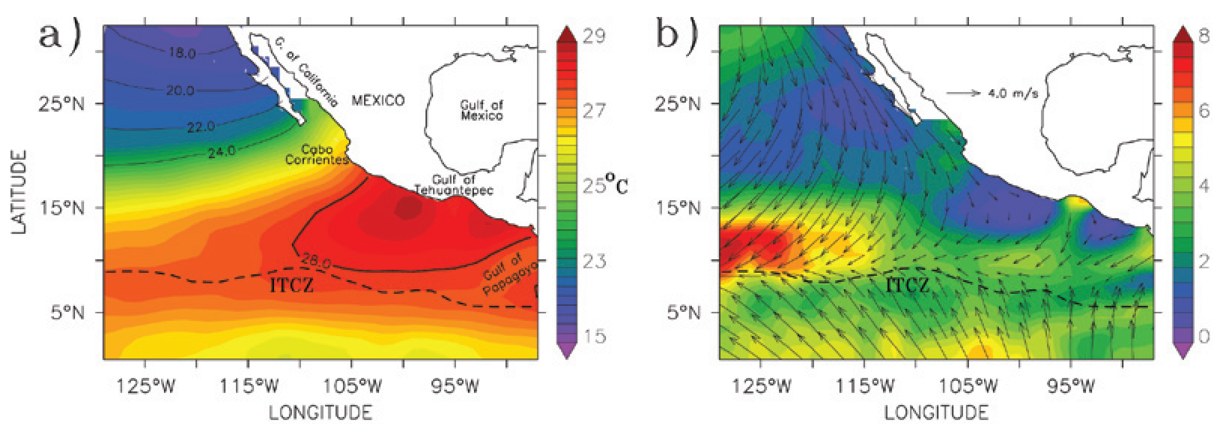

Fig. 1. a) Average temperature (oC) and b) variance of the wind velocity (color contours) and in vectors the average values. In both figures, the dotted line represents the approximate position of the ITCZ.

Data and Methods

The study area extends from 2° N to 35° N and from 130° W to 87° W (Fig. 1a). To study the relationship between the SST and the wind for long time scales, monthly data for 20 years of SST and wind measurements from Comprehensive Ocean–Atmosphere Data Set (COADS) were analyzed for the period between 1 January 1978 and 31 December 1997. These data are available from; http://ingrid.ldeo.columbia.edu/SOURCES/.COADS/.

For the analysis of propagation and of the relationship of the SST with equatorial currents, weekly sea surface heights (SSH) were used, derived from TOPEX/Poseidon (T/P) Generation-B Merged Geophysical Data (MGDR-B) corresponding to the period December 1992 to June 2002 (see http://www.aviso.oceanobs.com/en/data/products/sea-surface-height-products/global/msla/).

Temperature and salinity fields from the LEVITUS Climatology project (Levitus and Gelfeld, 1992; http://ingrid.ldeo.columbia.edu/SOURCES/.LEVITUS/) together with SSH of T/P were used to calculate the geostrophic currents of the zone.

With the aim of facilitating comparisons between the different databases, these were objectively interpolated onto a regular grid (x, y, t) of 1° × 1° × 1 month. We used a Gaussian correlation function with an influence radius of 700 km and influential time window of 70 days (for a description of the method see e.g., Bretherton *et al*., 1976; Carter and Robinson, 1987). All the analyses were done on the anomalies with respect to the temporal mean. To avoid contaminating the seasonal signal in the CCS with the highly energetic seasonal signal of the Gulf of California (e.g., wrongly averaging its value through the peninsula), data from the Gulf were removed from the analysis prior to the objective interpolation.

The spatial-temporal structure of the SST and wind anomalies was analyzed using Empirical Orthogonal Functions (EOF), constructing a covariance matrix of the SST anomalies and then solving an eigenvalue problem (Chelton, 1983). To explore the temporal variation of SST in the frequency space, the annual and semiannual harmonics were calculated.

To identify propagating structures, Complex Empirical Orthogonal Functions (CEOFs) were calculated, obtaining modes that relate the phase with the spatial field. The time-series used to calculate the CEOFs were built from the original series (e. g. SSH) plus their Hilbert transformation (see Barnett, 1983). With this series, the covariance matrix is calculated and the same mathematic procedure like for traditional EOFs is applied. The magnitude and the phase that correspond to each mode of the CEOFs can be calculated from the real and imaginary parts. To find the propagation velocity it is only necessary to calculate the slope of the spatial and temporal phase for each mode.

Results and Discussions

Average and annual SST

Fig. 1 shows the temporal average of the entire database for the SST and the winds field. For the SST (Fig. 1a) the maximum temperature coincides roughly with the ITZC west of 110° W but not to the east. There are local minima of SST in the Gulf of Tehuantepec and in the Gulf of Papagayo, which attenuate toward the southwest. The colored contours in Fig. 1b show the variance of the wind velocity, and the vectors represent its average values. On average, the cross-equatorial flow is from the south in the east of the region and becomes increasingly southeasterly as one moves west. The maximum wind variability is far to the west at 8˚ N-13˚ N; connected with the jets of the Gulfs of Tehuantepec and Papagayo along ~11˚ N by a narrow band of relatively high variability.

The harmonic analysis for SST shows an absolute maximum in the amplitude for the annual frequency (Fig. 2a) that extends northward from the mouth of the Gulf of California along the coast of Baja California (~25° N). This maximum amplitude can be considered as the combination of three factors: 1) the seasonal variability of the California Current, 2) the seasonal variability of the Gulf of California (Wyrtki, 1967), and 3) the seasonal presence of warm water pulses associated to tropical waters (Trasviña A., 2009; personal communication). Moreover the contours for the annual frequency are in agreement, in magnitude and form, with the reported by Soto-Mardones *et al* (1999); where the annual amplitude of the SST increase northward to the Gulf of California and the maxima in the zones of the mouth and adjacent to peninsula are the continuation of this maxima (Fig. 2a). Not only is the amplitude of the annual signal high in this zone but it also contains the highest SST variability, in Fig. 2b the percentage of the total variance explained by this frequency is shown. For the coastal zone near the mouth of the Gulf of California and for the west of the peninsula, the annual frequency contributes more than 80% of the total variance (Fig. 2b). Another zone of important activity in the annual frequency variation is the Gulf of Tehuantepec. In this region the amplitude of the annual signal is about half that of the mouth of the Gulf of California and it is also the most important component, since it explains more than 80% of the total variance there (Fig. 2b). The harmonic of the SST for the semi-annual frequency (not shown), is similar to the annual one but the explained percentage of the variance is much smaller.

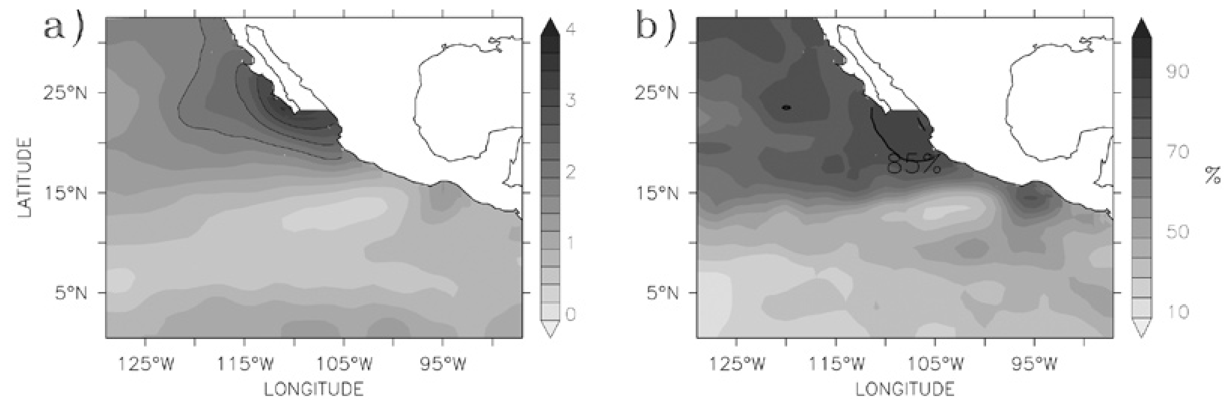

Fig. 2. a) Amplitude and b) percentage of the explained variance for the SST annual frequency.

Fig. 3 shows the EOF first mode of the variability for SST anomalies, including the annual signal (data are standardized, e.g., the temporal average is subtracted and the remainder divided by the standard deviation); this mode represents 58.55% of the total variability. In its spatial structure (Fig. 3a), it can be seen how the main form of variability of the SST is given as a latitudinal oscillation with its axis approximately at latitude 10° N (zero-value contour). Its associated time-series (Fig. 3b) shows an almost purely annual variation. This mode obviously extracts the dominant signal, which is that from solar heating. Moreover, in this mode it is observed, as in the harmonic analysis, that there is a maximum in the region near the mouth of the Gulf of California, again providing evidence of the importance of the contribution of the seasonal variability of the California Current, Gulf of California and the tropical current intrusion to the annual heating of this portion of the Pacific (Fig. 3a, b). The rest of the EOF modes are not shown here, since the percentage of the variability is small and do not cover any zones of significant variability.

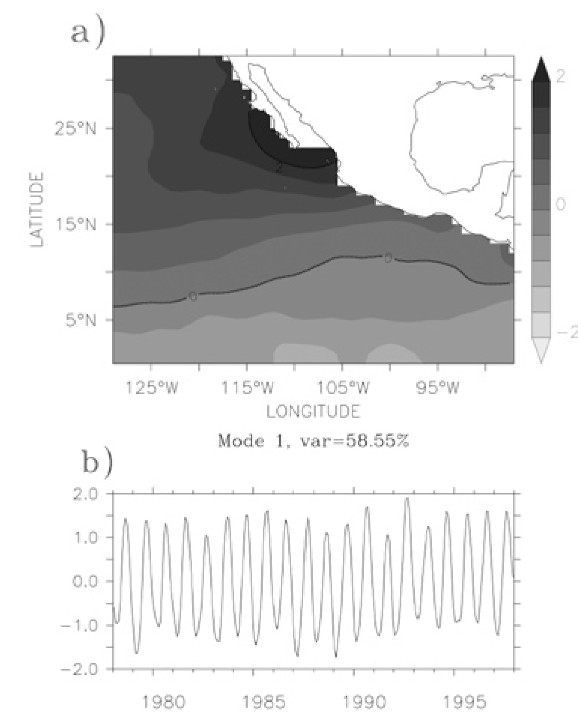

Fig. 3. First mode of the EOFs for the SST anomalies from COADS, including the annual signal: a) represents the spatial structure and b) is the time-series. Data are standardized so there are no units (see text).

SST and wind

For each point of the grid the correlation was calculated between the SST and the magnitude of the wind speed as shown in fig. 4. The zones of higher correlation are in front of both the Gulf of Tehuantepec and Cabo Corrientes. From the correlation of the SST with each of the components of the wind, we found that for the meridional component (Fig. 5a) there are two zones of maximum correlation, one in the Gulf of Tehuantepec and the other off Cabo Corrientes; while for the zonal component (Fig. 5b) there is only one maximum in Cabo Corrientes. It is evident that these maxima mark the important upwelling zones. For the Gulf of Tehuantepec the influence of the "Nortes" winds with a mainly meridional component, dominate the variability of the wind and in consequence the response of the ocean to these. For the zone off Cabo Corrientes, upwelling is produced by winds parallel to the coast (direction NW–SE), and therefore both components are highly correlated with the SST.

EOF analysis of two joint variables

The EOF analysis of two joint variables consists of testing these as a single one; that is, after standardizing both series (subtracting their respective temporal averages and dividing by their standard deviation), a single covariance matrix is formed, which links together these two matrices and can be analyzed using the same methodology as that used for traditional EOFs. Two spatial maps are generated from this analysis, which belong to each of the involved variables (in our case the SST and the wind). For a given mode, the areas where the absolute maxima coincide in these two spatial maps indicate the zones where the signals co-vary and its time-series contains information about the variation common to both variables (i.e., it contains the temporal variability that is common to the SST and the wind). The percentage of the explained variance denotes the relative importance of such common variability.

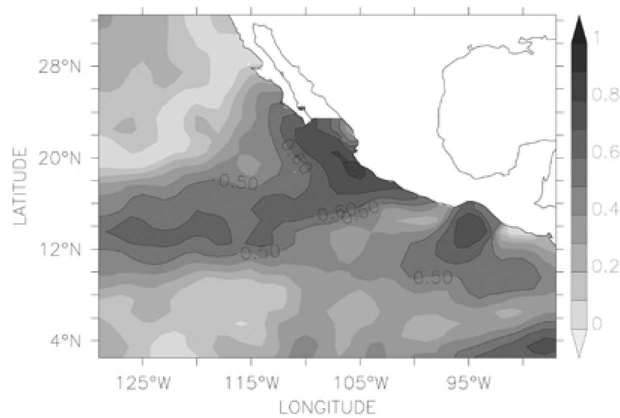

Fig. 4. Spatial correlation between the SST and the magnitude of the wind.

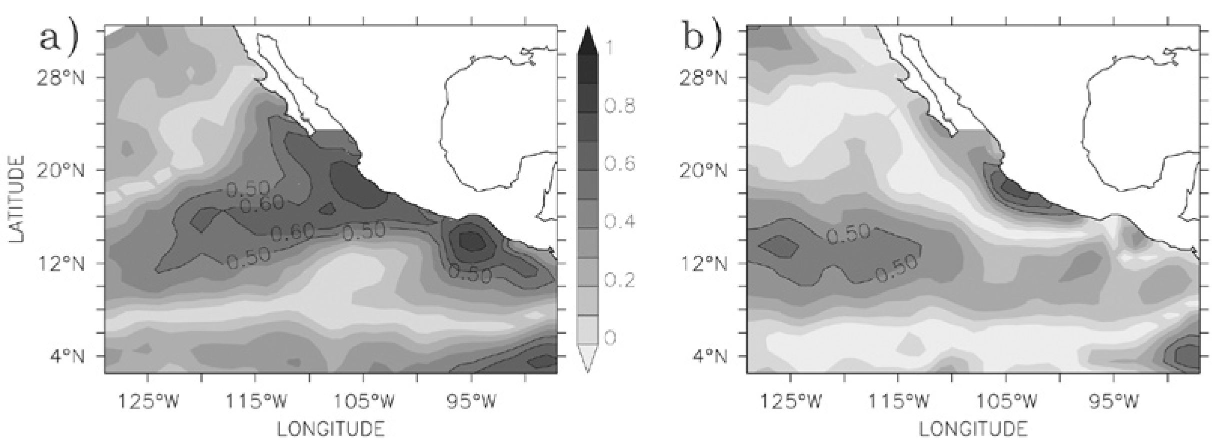

Fig. 5. Spatial correlation between the SST and the a) meridional and b) zonal components of the wind.

Fig. 6a and 6b show the spatial maps of the first mode for the SST and the magnitude of the wind, respectively. The first mode explains 34% of the total variability. Note the band of low variability (SST and wind) roughly corresponding with the Inter-Tropical Convergence Zone (ITCZ). To the north of 10° N the 1st mode shows high SST variability generally while it decreases quickly again in wind modulus north of Cabo Corrientes. Moreover for both variables, to the south of 4° N there is high variability, especially in the east of the area. The zones of common variation between SST and the magnitude of wind are given from 10° N to 20° N (off Cabo Corrientes) and near to equatorial zone. For this mode the temporal variation is basically annual (see Fig. 6c). In both regions the correlation is antisymmetric (180° out of phase); that is, when the wind anomaly is maximal, the SST anomaly is minimal, and vice versa. In the equatorial zone, as an example, this implies that when winds weaken (minimal anomaly, west winds diminish) temperatures rise, and vice versa. The same happens for the zone off Cabo Corrientes. North of 20° N there seems to be no correlation between the SST and the wind (i.e., the wind does not contribute to the seasonal variability of the SST). This suggests that the Gulf of California and not the wind is responsible for the maximum of the annual variability in the SST around the tip of the peninsula.

The second mode still contains an important part of the total variability (~18%). The temporal variation of this second mode (Fig. 7c) shows mainly an annual frequency; however, a small semiannual contribution can also be observed. In the spatial part (Fig. 7a, b), it can be seen that the zones of higher covariance are the Gulfs of Tehuantepec and Papagayo, and off the coast of Baja California. In a similar way to the first mode, this also represents an antisymmetric covariation; that is, positive

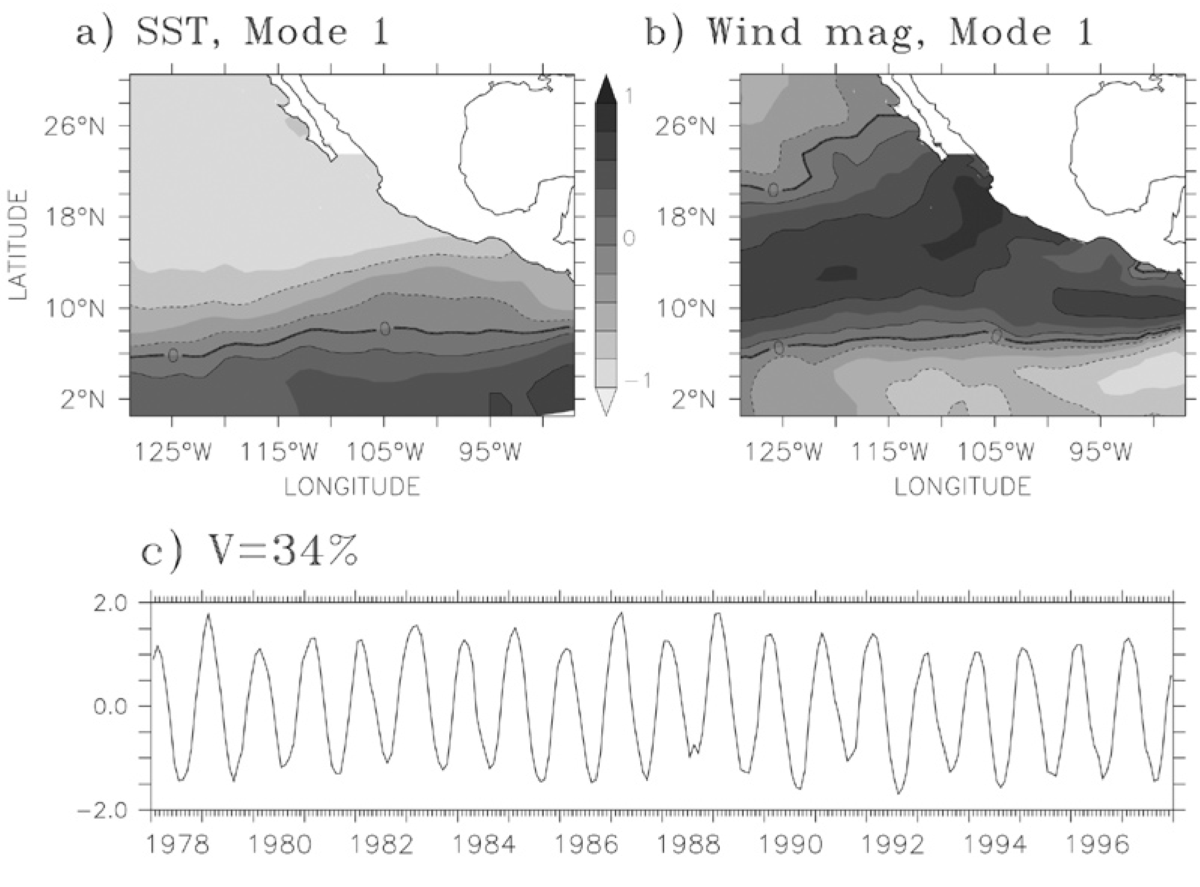

Fig. 6. First mode of the joint EOFs of a) SST and the b) wind magnitude. c) Time-series of the co-variability of the SST and the wind magnitude. V represents the percentage of the explained variance for this mode.

anomalies of one variable are linked with negative ones of another (e.g., strong winds with low temperatures), pointing to a coastal upwelling as the mechanism responsible for such co-variation off Baja California. The low temperatures in the Gulfs of Tehuantepec and Papagayo are also predominantly caused by intense wind though not through upwelling but by wind induced vertical mixing. The presence of a semiannual component also suggests an upwelling mechanism, since the magnitude of the wind (and not its components) has this frequency too; this is in agreement with the literature, as for the coast of Baja California it is well known that upwelling is caused by constant winds flowing along the coast (Amador, 1978; Gómez Váldez, 1980). For the Gulf of Tehuantepec, the mechanism that causes surface cooling also is due to wind. Although these winds are intermittent, they can produce areas of enhanced biological production (Lluch-Cota *et al*, 1997; Pennington *et al*, 2006).

Due to the fact that the percentages of the variance explained by the third and fourth modes are small compared with the first two, they are not shown here; but it is important to point out that each of these relate to the co-variation modes of a specific zone. For the third one, which explains only 4% of the total variability, the common zone of variation is off Baja California and seems to be associated with upwelling in the zone. The same occurs with the fourth mode, except that the common co-variation zone is the Gulf of Tehuantepec (with a variability percentage of 3%); it is evident that this mode is isolating the contribution to the SST by upwelling caused by the "Nortes".

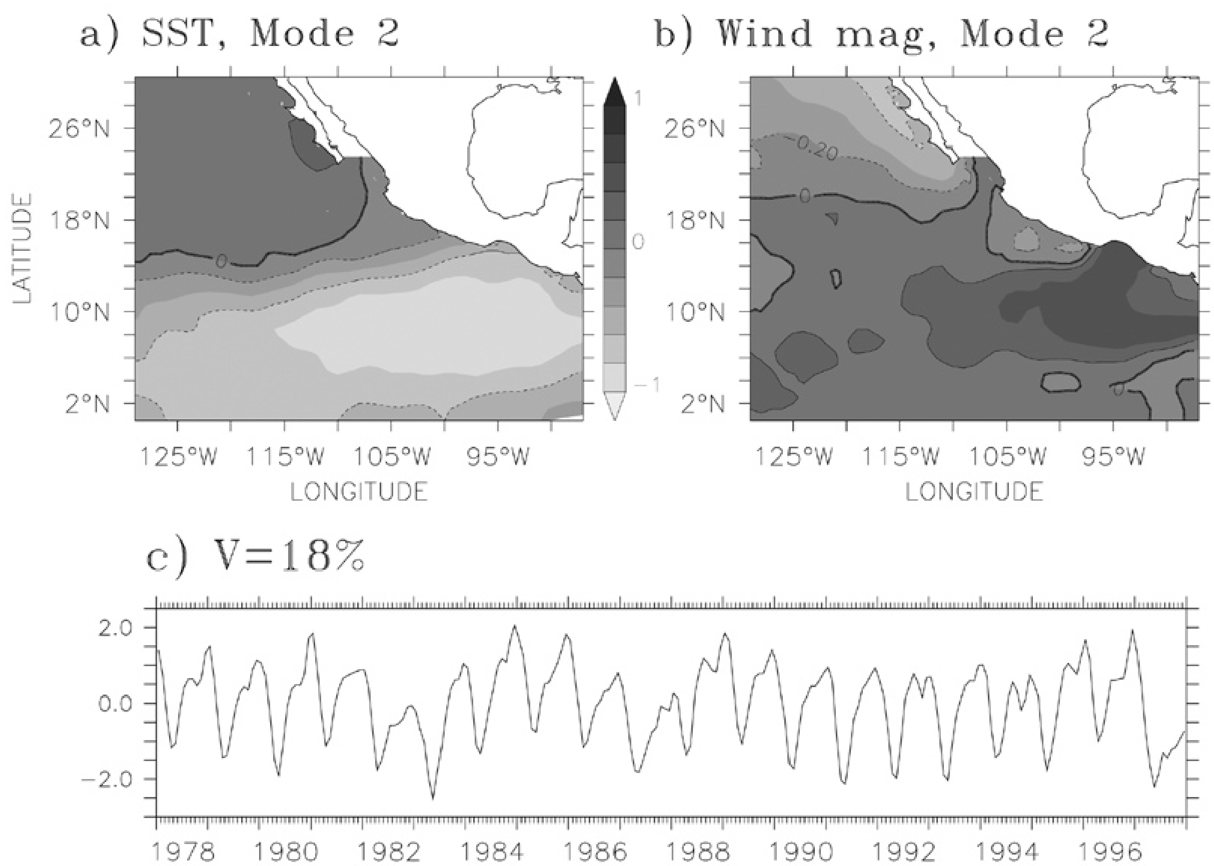

Fig. 7. Second mode of the joint EOFs of a) SST and the b) wind magnitude c) Time-series of the co-variability of the SST and wind magnitude. V represents the percentage of the explained variance for this mode.

Remote propagating signals

It has been shown that SSH signals propagate eastward and poleward in the form of equatorial and coastal Kelvin waves respectively (Enfield and Allen, 1980; Chelton and Davis, 1982). This same behavior has been describes for the SST [e.g., Lluch-Cota *et al*., 2001; Lluch-Cota *et al*., 2003]. Variability of the upper layer thickness associated to the passing of these waves is probably the link between these signals and SST, though a more or less effective Ekman Pumping mechanism (Parés-Sierra and O'Brien, 1989). To investigate this contribution and its possible influence on the seasonal variation of SST, CEOFs of TOPEX/Poseidon SSH data were constructed. The analyzed data go from 20 March 1993 to 1 March 2002 in 10-days intervals.

Fig. 8 shows the first mode of the CEOFs decomposition. This mode explains 66% of the total variability. Colors represents the amplitude and the phase is shown in contour lines (shown only where the amplitude is high, i.e., where the signal is important). The value of the contours is presented in degrees, and it decreases from the west along the equator and to the northwest along the coast (in this case these are negative numbers). This suggests that this signal is an equatorial Kelvin wave, which upon finding the coast, propagates toward the northwest as a coastal Kelvin wave. Fig. 8b and 8c show the phase and the magnitude for this mode, respectively. As is shown in the fig. 8c, the magnitude was highest around 1997, when the SSH was highest due to the strong El Niño of that year. The estimated propagating velocity of this phenomenon is 0.57 m s^{-1} which is within the typical velocities for Kelvin waves, which for this regions range from 0.5 to 3 m s^{-1}. The length of this event is approximately 43 months. In this mode not only is important the interannual signals, also it can remark the presence of the annual Kelvin waves propagating in the zone. These waves produce anomalous currents that move toward the north following the coast, causing the thermocline to sink. Both effects tend to raise the sea level and, as a consequence, the SST; the first one by bringing warm water from the west and the second one by isolating the cold, subsurface layer from the Ekman layer.

The spatial structure of the second mode (Fig. 9a) identifies a zonal area or propagation channel within 10° N and 15° N. It manifests itself as a maximum of amplitude. The phase (contour lines) increases from east to west, evidencing signals that propagate toward the west along this band. The phase and amplitude time-series for this mode indicate that such events occur annually (Fig. 9b, c) with an approximate velocity of 14 cm s^{-1}. Some authors suggest that these signals are anticyclonic eddies generated by local winds in the Gulfs of Tehuantepec and Papagayo, wich are more intense during winter. They have the same direction of propagation and approximately the same velocity as a baroclinic Rossby wave (15 cm s^{-1}; see Stumpf and Legeckis, 1977). Other authors, such as Hansen and Maul (1991), mention that these eddies probably form by variations of the North Equatorial Countercurrent (NECC), which during autumn and winter, flow eastward and turn northward after encountering the continent, allowing eddies propagating westward by a Rossby-wave-like mechanism, with velocities of 15 cm s^{-1}. However they recognize that this velocity is higher than that expected for Rossby waves, so the mechanism responsible for their advection must be different.

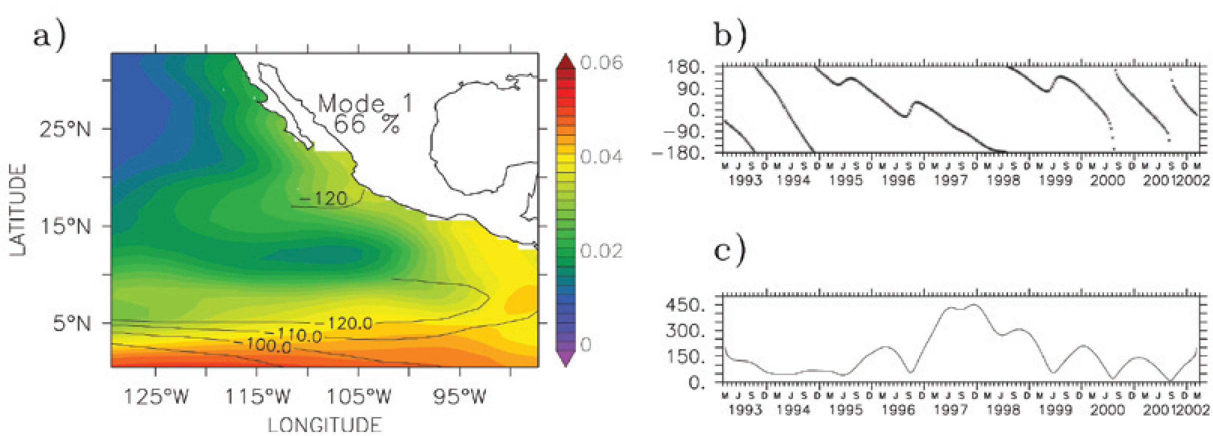

Fig. 8. First mode of the complex EOFs of the sea surface heights from T/P, a) the color represents the amplitude of the signal (in cm) and in contours the phase in degrees (in this case the values for the contours are negative). b) Phase (in degrees) and c) magnitude (without units) of the time-series associated to the first mode.

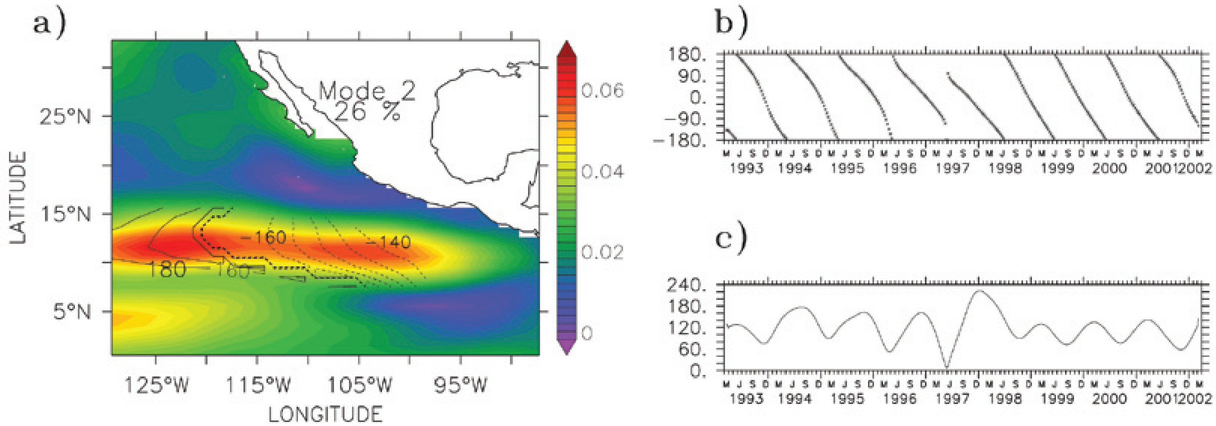

Fig. 9. Second mode of the complex EOFs of the sea surface heights from T/P, a) the color represents the amplitude of the signal (in cm) and contours represent the phase (in degrees). The dotted lines negative phase values and continuous lines are positive phase values. b) Phase (in degrees) and c) magnitude (whitout units) of the time-series associated with the second mode.

Fig. 10 shows the seasonal climatology of the geostrophic currents. To obtain these we first calculated dynamic heights and geostrophic currents from the LEVITUS Climatology, assuming 500 m depth as the level of no-motion. Then, from the monthly averages of SSH anomalies from T/P for the period January 1993 to December 2001, the mean was used to eliminate the residual error of the geoid, and surface velocities were calculated. Finally, to replace the subtracted mean, dynamic heights from LEVITUS Climatology were added to the surface velocities, thus obtaining the fields of geostrophic velocities for the zone. A similar method has been used by other authors to characterize the surface circulation in different regions (e.g., Lagerloef *et al.* (1999) for the equatorial Pacific and Strub and James (2002) for the northeast Pacific).

In figs. 9 and 10, there is a coincidence between the North Equatorial Current (NEC) and the belt of higher variability, which suggests a relation of advection between eddies generated in the Gulfs of Tehuantepec and Papagayo and the NEC, which is more intense during winter. The displacement velocity (~15 cm s^{-1}) of these gyres, as well as their temporality, show that the generation of eddies in the Gulfs of Tehuantepec and Papagayo, caused by instability processes and/or directly by wind forcing, together with their advection by the NEC, are responsible for the "conspicuous" belt of high variability (10°–15° N) and are, therefore, another of the important factors in the modulation of the seasonal variation of the SST in the ETP. The seasonal variability of the Equatorial Current System and the existence of this high-variability belt can be described as follows (see fig. 9a and 10):

- During autumn (November), the NECC is strong; the NEC is located at its northernmost position (15°N).

- During winter (February), the system moves south: the NECC is still present but at around 5° N, and the NEC is well developed at around10 N with velocities between 15 and 25 cm s^{-1}. To the north of the NEC there appears some return flow eastwards that combines with the California Current.

- During spring (May), the NECC weakens and is detectable only around 5°N in the western part, the NEC is stronger and well formed all over the domain around 8–12°N, with velocities between 20 and 25 cm s^{-1} and the return flow north of it has also intensified.

- During summer (August), the NECC begins to develop at around 6° N. Note that south of 5°N the South Equatorial Current is present, as in November and May, and the NEC is absent.

It is important to remark, that similar patterns have been shown in recent climatologies (Strub and James, 2002; Kessler 2002, 2006).

ITCZ and the thermal equator

In the southern part of our domain, the evolution of the ITCZ also modulates the SST, including the position of the thermal equator. We computed the average seasonal position of the ITCZ and the thermal equator in the following way: first we calculated the climatology of the zonal and meridional components of the wind velocity from the 20 years of COADS data. Then, at each longitude, looked for the nearest position to the equator where the divergence was equal to zero, and averaged from 130° W to 87° W (i.e., along our longitudinal domain). Finally, the temporal evolution of this averaged latitudinal position of the ITCZ was plotted in fig. 11. The position of the thermal equator was calculated in a similar way; that is, the highest value of SST that was found nearest the equator for each time and averaged longitudinally. It is also plotted on fig. 11.

From Fig. 11 it can be seen that the ITCZ reaches its northernmost position (~10° N) during summer and its southernmost position (~6° N) during winter. The temporal evolution of the ITCZ has the same form as that of the position of the thermal equator, which is in agreement with Barnett (1977). The position of the latter is found at approximately 4° north of the ITCZ, delimiting part of the southern boundary of the Tropical Western Hemisphere Warm Pool (Curtis *et al.*, 2003). The reason for this latitudinal displacement lies in the fact that the position of the ITCZ is located in the region of confluence of the trade winds (Hastenrath, 1991), maximum convergence of masses and of maximum cover by convective clouds (high cloudiness; Amador, 2006), therefore inhibiting the solar radiation in this area and causing the maximum SST to be located a little north from the ITCZ. Given that the average position of the ITCZ is not always found at the same latitude, the position of the thermal equator also shifts.

Conclusions

The basic characteristic of the SST variability is due to solar heating. Temperature decreases from the thermal equator towards the poles and varies mainly annually. It was found that the most important factors that modulate this fundamental variability in the ETP are:

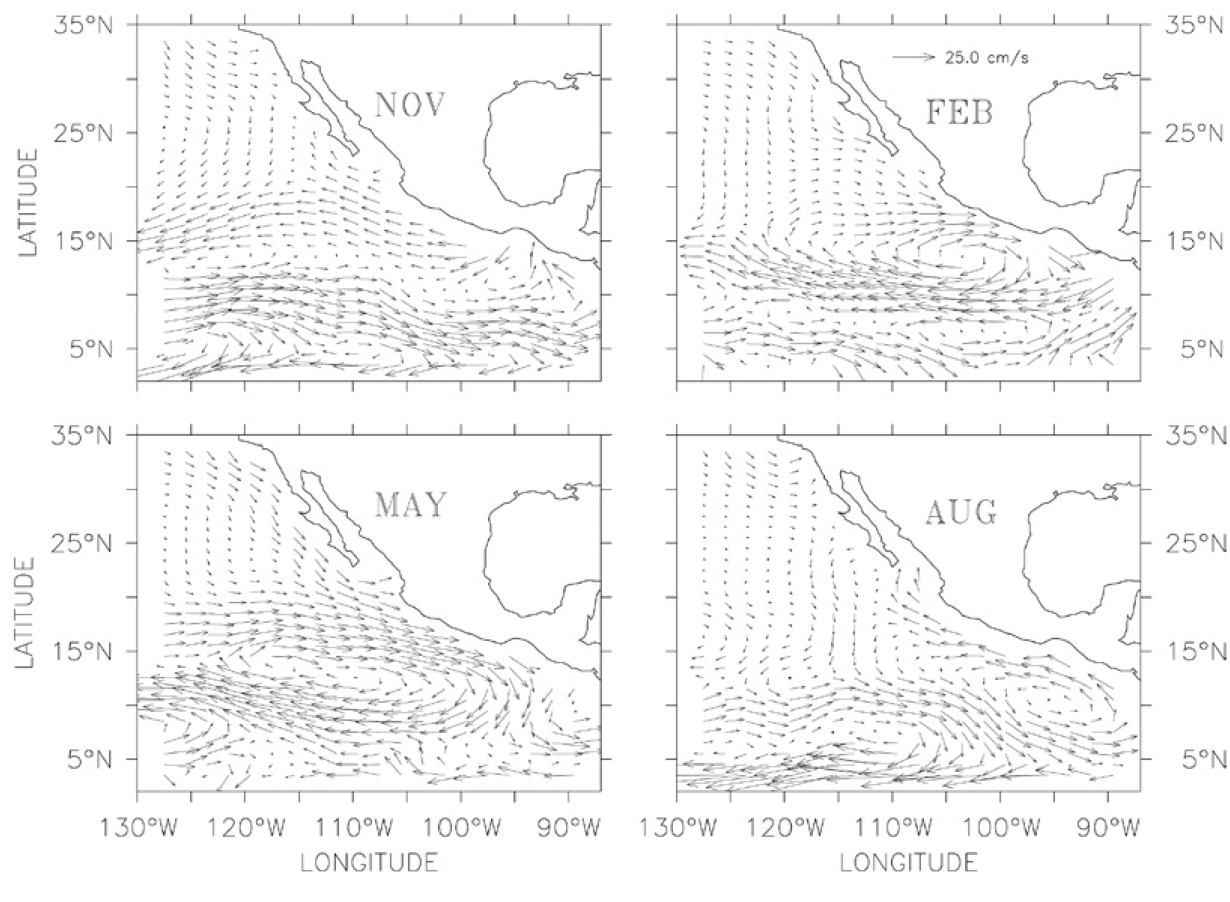

Fig. 10. Calculated geostrophic currents from the T/P data + LEVITUS Climatology for the indicated months.

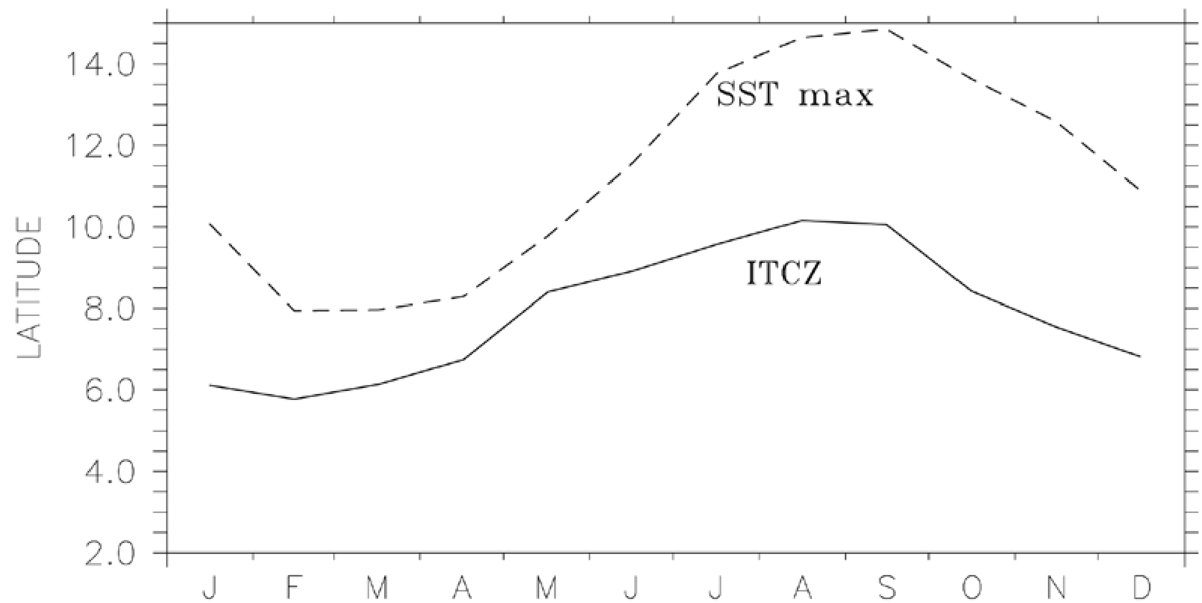

Fig. 11. Latitudinal position of the ITCZ and the maximum SST around the equator, averaged between 130° W–87° W.

- The influence of the variability of the California Current together with the Gulf of California and the possible presence of a Tropical current, that extend from the mouth of the gulf (24° N) toward the south approximately 200 km and toward the west and north, by the occidental coast of the peninsula approximately 300 km. This area has the most intense annual signal.

- The influence of the Gulf of Tehuantepec is another local factor that modulates the variability of the SST in the ETP. Its influence is mainly due to the behavior of the winds in the area. They are intense and perpendicular to the coast during winter, causing an anomalous cooling effect on the surface.

- Upwelling is another form of co-variability between the SST and the wind. For our study area the equatorial region, in front of Cabo Corrientes, west off Baja California, and the Gulf of Tehuantepec are the most relevant areas of seasonally modulated SST variability due to upwelling.

- The seasonal variation of the location of the thermal equator is evidently related to the position of the ITCZ. Its seasonal variation is another of the important factors of modulation of the SST of the Eastern Pacific at a seasonal scale.

- The presence of equatorial and coastal Kelvin waves is another important factor of SST modulation. These waves propagate mainly with an interannual period, (e.g. signal associated with the El Niño events for 1992 and 1997), but an annual component is also present.

- There is also a SST seasonal modulation by westward advection of SSH anomalies at about 10°N. Analyzing the SSH and SST anomalies in conjunction with the geostrophic currents we found that this westward displacement, at about 15–20 cm s^{-1}, most probably is due to advection of eddies by the NEC.

Acknowledgments

This work was supported by CONACYT (Mexico) through contract SEP2003-C0244534.

Bibliography

Alvarez, L. G., A. Badan-Dangon and A Valle, 1989. On coastal currents off Tehuantepec. Estuarine Coastal *Shelf Science*. *29*, 89-96.

Amador, A., 1978. Análisis de vientos, corrientes y nivel del mar en una zona de surgencias cerca de Punta Colonet. Thesis of master degree, CICESE, 32.

Amador, J. A., E. J. Alfaro, O. G. Lizano and V. O. Magaña, 2006. Atmospheric forcing of the eastern tropical Pacific: A review. Progress in Oceanography: A review of Eastern Tropical Pacific Oceanography. 69,101-142.

Badan-Dangon, A., 1998. Coastal circulation from the Galápagos to the Gulf of California. In: Robinson, A.R. and K.H. Brink (eds), The Sea, Vol. 11. John Wiley and Sons, New York, 315–343.

Barnett, T. P., 1977. The principal time and space scales of the Pacific Trade winds fields. *Journal of the Atmospheric Sciences. 34, 2*. 221-236.

Barnett, T. P., 1983. Interaction of the Monsoon and Pacific trade winds system at interannual time scales. Part I: The equatorial zone. *Monthly Weather Review. 11, 4*, 756-773.

Bretherton, F. P., R. E. Davis and C. B. Fandry, 1976. A technique for objective analysis and design of oceanographic experiments applied to MODE-73. *Deep Sea Research. 23*, 559–582.

Chelton, D. B. and R. E. Davis, 1982. Monthly mean sea level variability along the west coast of North America. *Journal of Physical Oceanography. 12*, 757-784.

Chelton, D. B., 1983. Effects of sampling errors in statistical estimation. *Deep Sea Research. 30(10A)*, 1083-1183.

Carter and A. R. Robinson, 1987: analysis models for the estimation of oceanic fields, *J. Atms. and Ocean. Techn., 4*, 49-74.

Clarke, A. J. and S. Van Gorder, 1994. On ENSO coastal currents and sea levels. *Journal of Physical Oceanography. 24*, 661–680.

Curtis, S., R. F. Adler and G. J. Huffman, 2003. A case of the Intertropical Convergence Zone at the ocean surface with high resolution satellite data. In: 12th Conference on Interaction of the Sea and Atmosphere, Long Beach, CA.

Enfield, D. B. and J. S. Allen, 1980. On the structure and dynamics of monthly mean sea level anomalies along the Pacific coast of North and South America. *Journal of Physical Oceanography. 10*, 557-578.

Fielder, P. C. and L. D., Talley, 2006. Hydrography of the Easern Tropical Pacific: A review. Progress in Oceanography: *A review of Eastern Tropical Pacific Oceanography. 69*, 143-180.

Gómez Valdez, J., 1980. Variación estacional en el sistema de la corriente de California frente a Ensenada, Baja California. Thesis of Master degree. CICESE, 165.

Hansen, D. V. and G. A. Maul, 1991. Anticyclonic current rings in the eastern tropical ocean. *Journal of Geophysical Research. 96*, 6965–6079.

Hastenrath S., 1991. Climate dynamics of the tropics. Kluwer Academic Pubishers, Dordrecht, 488.

Kessler, W. S., 2002. Mean three-dimensional circulation in the Northeast Tropical Pacific. *Journal of Physical Oceanography. 32*, 2457-2471.

Kessler, W. S., 2006. The circulation of the Eastern Tropical Pacific: A review. Progress in Oceanography: *A review of Eastern Tropical Pacific Oceanography. 69*, 181-217.

Lagerloef, G. S. E., G. T. Mitchum, R. B. Lukas and P. P. Niiler, 1999. Tropical Pacific near-surface currents estimated from altimeter, wind and drifter data. *Journal of Geophysical Research. 104*, 23313–23326.

Levitus, S. and R. Gelfeld, 1992. NODC Inventory of physical Oceanographic profiles, key to oceanography records documentation, No. 18. NODC, U.S Gov. Printing office. Washington. D. C.

Lluch-Cota, D. B., W. S. Wooster and S. R., Hare, 2001. Sea surface temperature variability in coastal areas of the Northeastern Pacific related to El Niño-Southern Oscillation and the Pacific Decadal Oscillation. *Geophysical Research Letters. 28*, 2029-2032.

Lluch-Cota, D. B., W. S. Wooster, S. R., Hare, D., Lluch-Belda and A. Parés-Sierra, 2003. Principal modes and related frequencies of the sea surface temperature variability in the Pacific coast of North America. *Journal of Oceanography. 59*, 477-488.

Lluch-Cota, S. E., S. Alvarez-Borrego, E. M.Santamaria del Angel, F. E. Müller-Karger and S. Hernández-Vázquez, 1997. The Gulf of Tehuantepec and adjacent areas: Spatial and temporal variation of satellite-derived photosynthetic pigments. *Ciencias Marinas. 23*, 329-340.

Magaña, V., J. Amador, and S. Medina, 1999. Midsummer drought over Mexico and Central America. *Journal of Climate.12*, 1577-1588.

Magaña, V. O. and E. Caetaño, 2005. Temporal evolution of summer convective activity over the Americas warm pools. *Geophysical Research Letters. 32*, 2.

Parés-Sierra, A. and J. O'Brien, 1989. The seasonal and interannual variability of the California Current System: a numerical model. *Journal of Geophysical Research. 94*, 3159–3180.

Parés-Sierra, A., M. López-Mariscal and E. Pavía-López, 1997. Oceanografía del Océano Pacífico Nororiental. In: Lavín, M.F. (ed.), Contribuciones a la Oceanografía Física en México, Monografía No. 3, UGM, 1–24.

Pennington, J. T., K. L. Mahoney, V. S. Kuwahara, D. D. Kolber, R. Calienes and F. P Chavez, 2006. Primary production in the eastern tropical Pacific: A review. Progress in Oceanography: *A review of Eastern Tropical Pacific Oceanography. 69*, 285-317.

Philander, S. G., 1990. El Niño, La Niña and the Southern Oscillation. International Geophysics Series, Vol. 46. Academic Press, San Diego, CA.

Romero-Centeno, R., J. Zavala-Hidalgo, A. Gallegos and J. J. O'Brien, 2003. Isthmus of Tehuantepec wind climatology and ENSO signal. *Journal of Climate; Notes and Correspondence. 16*, 2628-2639.

Soto-Mardones, L., S. G. Marinone and A. Parés-Sierra, 1999. Time and spatial variability of the sea surface temperatura in the Gulf of California. *Ciencias Marinas. 25*, 1, 1-30.

Strub, P. T. and C. James, 2002. Altimeter-derived surface circulation in large-scale NE Pacific Gyres. I. Seasonal variability. *Progress in Oceanography. 53/2-4*, 163-183.

Stumpf, H. G. and R. V. Legeckis, 1977. Satellite observations of mesoscale eddy dynamics in the eastern tropical Pacific Ocean. *Journal of Physical Oceanography. 7*, 648–658.

Trasviña A. and E. D. Barton, 1997. Los Nortes del golfo de Tehuantepec: la circulación costera inducida por el viento. Contribuciones a la oceanografía física en México. *Monografia 3*, Unión Geofísica Mexicana, 1997. 25-46.

Trasviña, A., E. D. Barton, J. Brown, H. S. Velez, P. M. Kosro and R. L. Smith, 1995. Offshore wind forcing in the Gulf of Tehuantepec, México: The asymmetric circulation. *Journal Geophysical Research. 100, 20*, 649-663.

Wang, C. and D. B. Enfield, 2001. The Tropical Western Hemisphere Warm Pool. *Geophysical Research Letters. 28*, 1635–1638.

Wang, C. and D. B. Enfield, 2003. A further study of the Tropical Western Hemisphere Warm Pool. *Journal of Climate. 16*, 1476-1493.

Wyrtki, K. 1965. Surface Currents of the Eastern Tropical Pacific Ocean. Inter-American Tropical Tuna Commission. *Bullentin 9. 5*. 271-304.

A. L. Flores-Morales*, A. Parés-Sierra, S. G. Marinone
Departamento de Oceanografía Física, Centro de Investigación Científica y Educación Superior de Ensenada, A. P. 2732, Ensenada, B. C., Mexico.
**Corresponding author: alflores@cicese.mx*